INFECTION AND IMMUNITY, Mar. 2009, p. 1230–1237 Vol. 77, No. 3
0019-9567/09/$08.00+0 doi:10.1128/IAI.01117-08

Role of the *dosR-dosS* Two-Component Regulatory System in *Mycobacterium tuberculosis* Virulence in Three Animal Models▽†

Paul J. Converse,[1]* Petros C. Karakousis,[1] Lee G. Klinkenberg,[1] Anup K. Kesavan,[1] Lan H. Ly,[2] Shannon Sedberry Allen,[2]‡ Jacques H. Grosset,[1] Sanjay K. Jain,[1] Gyanu Lamichhane,[1] Yukari C. Manabe,[1] David N. McMurray,[2] Eric L. Nuermberger,[1] and William R. Bishai[1]

Center for Tuberculosis Research, Johns Hopkins University School of Medicine, Baltimore, Maryland,[1] and Department of Microbial and Molecular Pathogenesis, Texas A&M University System Health Science Center, College Station, Texas 77843[2]

Received 6 September 2008/Returned for modification 11 October 2008/Accepted 14 December 2008

The *Mycobacterium tuberculosis dosR* gene (Rv3133c) is part of an operon, Rv3134c-Rv3132c, and encodes a response regulator that has been shown to be upregulated by hypoxia and other in vitro stress conditions and may be important for bacterial survival within granulomatous lesions found in tuberculosis. DosR is activated in response to hypoxia and nitric oxide by DosS (Rv3132c) or DosT (Rv2027c). We compared the virulence levels of an *M. tuberculosis dosR-dosS* deletion mutant (Δ*dosR-dosS* [Δ*dosR-S*]), a *dosR*-complemented strain, and wild-type H37Rv in rabbits, guinea pigs, and mice infected by the aerosol route and in a mouse hollow-fiber model that may mimic in vivo granulomatous conditions. In the mouse and the guinea pig models, the Δ*dosR-S* mutant exhibited a growth defect. In the rabbit, the Δ*dosR-S* mutant did not replicate more than the wild type. In the hollow-fiber model, the mutant phenotype was not different from that of the wild-type strain. Our analyses reveal that the *dosR* and *dosS* genes are required for full virulence and that there may be differences in the patterns of attenuation of this mutant between the animal models studied.

Tuberculosis control is complicated by the ability of *Mycobacterium tuberculosis* to persist in human tissues despite host immune containment. Low oxygen tension occurring in granulomatous lesions and/or nitric oxide (NO) exposure due to macrophage activation may be an important factor in promoting mycobacterial persistence. The *M. tuberculosis* dormancy survival regulator (*dosR* [*devR*]) (3) encoded by Rv3133c is a member of a two-component regulatory system that is induced by hypoxia and NO exposure and may be an important transcriptional regulator during persistence. The sensor component is encoded by *dosS* (Rv3132c), although DosR can also be activated by an alternate sensor encoded by *dosT* (Rv2027c).

No animal model perfectly mimics the spectrum of human tuberculosis (4). The mouse model is inexpensive, well characterized, reproducible, and capable of demonstrating the sterilizing activity of rifampin and pyrazinamide on persisting tubercle bacilli (16). However, mouse granulomas are diffuse cellular aggregates (28) that are histologically distinct from human caseous granulomas. Guinea pigs and rabbits reproducibly form classical-appearing caseous granulomas (37), which, in rabbits, may subsequently liquefy and cavitate (8). While precise oxygen tension measurements have not been determined for tuberculous lung lesions in these three species, there is recent evidence that the granuloma-like lesions in mouse lungs lack tissue hypoxia (2, 36). In contrast, oxygen levels may be more profoundly depleted within guinea pig (17) and rabbit (38) lesions, which more closely approximate the histology of human tuberculous lesions.

The *dosR* gene is induced following exposure to progressive hypoxia in vitro (39) and might be required for *M. tuberculosis* survival in the hypoxic lesions of guinea pigs or rabbits. *Mycobacterium bovis* BCG lacking *dosR* is attenuated under hypoxic conditions in vitro (3). However, *dosR* is also induced in response to NO (29, 39), which is likely a major factor in *M. tuberculosis* growth containment in the mouse. The transcriptional response of bacteria to either hypoxia or NO appears to have significant, if not complete, overlap (4, 33). Therefore, all three animal models have the potential to be informative regarding the importance of the DosR regulon during *M. tuberculosis* infection.

Previously reported studies using the mouse (26, 31) and guinea pig (21) models have produced conflicting results regarding the virulence of *M. tuberculosis* lacking *dosR*. Parish et al. previously found that SCID mice infected intravenously with a *dosR* deletion mutant died more rapidly than mice infected with wild-type bacteria (26). Mutant-infected DBA/2 mice also had higher organ bacterial burdens. Rustad et al., on the other hand, observed similar levels of growth of H37Rv and the Δ*dosR* mutant in organs from three mouse strains (31). However, Malhotra et al. found that a mutant expressing a truncated DosR protein showed reduced pathology and spleen bacillary burdens in subcutaneously infected guinea pigs (21).

Given the conflicting phenotypes observed for different *dosR* mutants in mice and guinea pigs, we sought to test directly the role of *dosR* in *M. tuberculosis* virulence in different animal models with various degrees of resistance to *M. tuberculosis* infection. Using the resources of the Tuberculosis Animal Research and Gene Evaluation Taskforce (http://webhost.nts.jhu.edu/target/), we evaluated bacterial load over time, mortality,

* Corresponding author. Mailing address: Center for Tuberculosis Research, 1550 Orleans Street, Room 103, Baltimore, MD 21231. Phone: (410) 502-8236. Fax: (410) 614-8173. E-mail: pconvers@jhsph.edu.

† Supplemental material for this article may be found at http://iai.asm.org/.

‡ Present address: Department of Medicine, Division of Infectious Diseases, Vanderbilt University School of Medicine, Nashville, TN.

▽ Published ahead of print on 22 December 2008.

gross pathology, and histopathology of mice, guinea pigs, and rabbits infected by aerosol with the same *M. tuberculosis* H37Rv strain, a deletion mutant lacking *dosR* and *dosS* (Δ*dosR-S*) in which a single deletion event resulted in the deletion of adjacent genes, and a *dosR*-complemented strain (Comp). We also tested these strains in a mouse hollow-fiber (HF) model of tuberculosis (12), which was recently shown to develop tissue hypoxia (14). Because the Δ*dosR* strain was reported to be hypervirulent in the mouse model (26) and rabbits are relatively resistant to infection with wild-type *M. tuberculosis*, hypervirulence associated with *dosR* deficiency should be readily apparent in the rabbit model. However, our results consistently show an attenuated phenotype for the Δ*dosR-S* deletion mutant in the aerosol models but also phenotypic differences between the various models.

MATERIALS AND METHODS

Mycobacteria and culture conditions. Subcultures of H37Rv, H37Rv:Δ*dosR*::*kan*, and Comp were prepared from frozen stocks (obtained from D. Sherman, University of Washington) in Middlebrook 7H9 broth with 0.1% Tween 80 and 10% oleic acid-albumin-dextrose-catalase (Becton Dickinson) or on Middlebrook 7H10 plates at 37°C, as described previously (34). When needed, kanamycin (20 μg ml^{-1}) and hygromycin (50 μg ml^{-1}) were added. All strains were passaged twice in BALB/c mice.

Bacterial strains. The targeted disruption of *dosR* was performed as described previously (34).

***dosR* complementation.** The *dosR* upstream region was PCR amplified using specific primers (see Table S1 in the supplemental material). The amplicon was cloned into the PvuII and Asp718 sites of a pMH108-based integrating vector (9) to generate the complementation vector pDosR. This construct was integrated into H37Rv:Δ*dosR* by electroporation (29). This strain, H37Rv:Δ*dosR*::*dosR*, is here referred to as Comp.

Progressive hypoxia model of infection and reverse transcription (RT)-PCR analysis. The progressive hypoxia model was performed as described previously (40). Methylene blue decolorization served as a visual indicator of oxygen levels corresponding to nonreplicating persistence stage 2 (40). Samples were collected from parallel cultures 3 days prior to the methylene blue color change. RNA was recovered from samples as previously described (34), confirmed to be DNA free, and stored at −80°C. cDNA was prepared using iQ Sybr green supermix (Bio-Rad) according to the manufacturer's recommendations and amplified by quantitative PCR using gene-specific primers (see Table S1 in the supplemental material). The cycle threshold value (C_T) obtained for each gene of interest was normalized with that of *sigA* (23) in order to obtain a normalized C_T [normalized C_T = (*sigA* C_T) − (C_T for gene of interest)]. Each value represents the average of data from three technical replicates.

Mice and infection with *M. tuberculosis*. Animal protocols were approved by the Johns Hopkins University Animal Care and Use Committee. Six-week-old female C57BL/6 and BALB/c mice (Charles River, Wilmington, MA) were infected with *M. tuberculosis* H37Rv, H37Rv Δ*dosR-S*, or Comp using the GlasCol (Terre Haute, IN) inhalation exposure system. CFU counts of the inoculum were determined. On day 1 after infection, three to five mice from each group were sacrificed, and the number of implanted CFU was determined. At regular time points thereafter, five mice from each group were sacrificed for lung and spleen CFU counts. Typically, half of each lung was used for CFU counts, and the other half was placed into formalin for histopathology. Additional mice in each group were monitored daily for time to death.

Guinea pigs and infection. Outbred Hartley guinea pigs (Charles River, Wilmington, MA) were maintained according to procedures of the Texas A&M University Laboratory Animal Care Committee. Guinea pigs were infected with approximately 20 CFU of *M. tuberculosis* H37Rv, H37Rv Δ*dosR-S*, or Comp in a Madison aerosol chamber, as described previously (41). Five animals from each group were sacrificed at 2 and 6 weeks after infection. The right lower lung lobe and a portion of the spleen were homogenized in separate Teflon-glass homogenizers and plated for CFU enumeration. Twenty-four hours prior to sacrifice, each guinea pig was injected with 100 tuberculin units (2 μg) of purified protein derivative (PPD) (Mycos, Loveland, CO) into a shaved area on the flank. Induration was measured 24 h later, and mean diameter was recorded.

Rabbits and infection. Female New Zealand White rabbits (Covance Research Products, Denver, PA) were maintained according to protocols approved by the Johns Hopkins University Animal Care and Use Committee, George Washington University, and the U.S. Army Medical Research Institute of Infectious Diseases (6). Infection was performed as described previously (22). For each rabbit, the number of viable bacilli inhaled was calculated based on the volume of inhaled air during exposure and the number of CFU cultured from the impinger samples per milliliter. Two days prior to sacrifice, Old Tuberculin concentrate (Wyeth Lederle, Pearl River, NY) was injected intradermally, and induration was measured as previously described (22). At day 1 and at 5 weeks (experiment 1) or at 8 weeks (experiment 2) after infection, the rabbits were sacrificed, and the number of grossly visible primary tubercles in the entire lungs was counted by Lurie's tubercle count method (7, 18). The right upper lobe was homogenized for determination of bacterial burden.

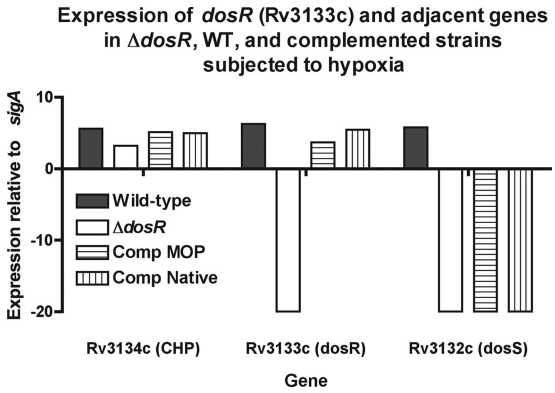

FIG. 1. Expression of components of the *dosR* operon (Rv3134c-Rv3132c). Four strains, the H37Rv wild-type (WT) parental strain (solid bars), a putative *dosR* deletion mutant, and two Δ*dosR*-complemented strains with native and mycobacterial optimal promoters (MOP), were subjected to hypoxic stress (see Materials and Methods) to enhance expression. Extracted DNA-free RNA was subjected to RT, and the cDNA was subjected to 40 cycles of quantitative PCR. Expression was normalized to that of the housekeeping gene *sigA* (~20 cycles), such that enhanced expression (fewer cycles to detection [C_T]) is shown as being positive and those with undetectable product are shown as being negative. The deletion mutant has no detectable *dosR* or *dosS*, while the complemented strains have restored *dosR* but not *dosS*.

HF assay. Infection with *M. tuberculosis*, the deletion mutant, or Comp strains was achieved using 6- to 8-week-old female hairless immunocompetent SKH1 mice (Charles River) using the HF encapsulation-implantation technique as described previously (12). For determinations of CFU counts, HFs were recovered from mice at the time of sacrifice (days 1, 7, 14, 21, 28, and 56). Log-transformed CFU values were used to calculate averages and standard errors.

Pathology and histopathology. Lungs and spleens (as well as guinea pig liver) were excised from all animals and stored in 10% formalin, embedded, and stained with hematoxylin and eosin for pathological analysis. In order to determine the extent of granulomatous tissue, the area of guinea pig lesions was measured using Image-Pro Plus 5.1 software.

RESULTS

RT-PCR analysis reveals the absence of both *dosR* and *dosS* from the Δ*dosR* strain. In vitro growth in a variety of media was measured to assess the fitnesses of the mutant strains. We determined that all four strains grew comparably in vitro (see Fig. S1 in the supplemental material). RT-PCR was used to verify the presence of *dosR* and the other components of its operon in the three strains, as well as in another *dosR*-complemented strain with a different promoter construct, after exposure to hypoxic stress, a condition known to induce *dosR* expression (39). RT-PCR revealed that all four strains carried the upstream gene Rv3134c (Fig. 1). As expected, Rv3133c (*dosR*) expression was absent only in the

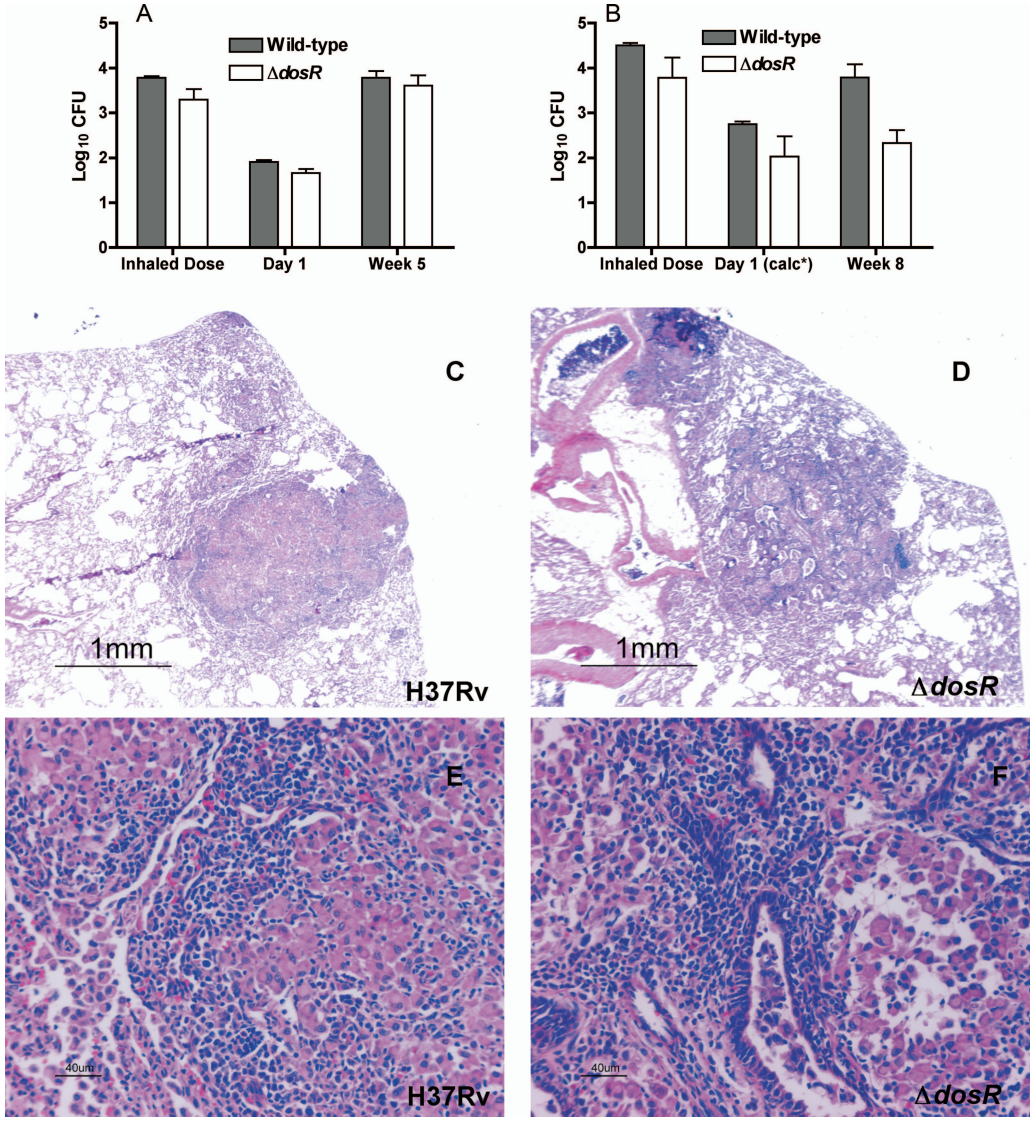

FIG. 2. Comparison of *M. tuberculosis* H37Rv:Δ*dosR-S* and wild-type H37Rv in rabbits after aerosol infection. In a first 5-week experiment (A), the bacterial burden was comparable at 5 weeks, while in a second 8-week experiment (B), there was a significantly ($P = 0.0312$ by Wilcoxon test) lower bacillary burden at 8 weeks. The average inhaled doses in each experiment were not significantly different between bacterial strains. The differences were also not significant with regard to the number of bacteria implanted (1.91 ± 0.04 $\log_{10}$ CFU for the wild type and 1.66 ± 0.097 $\log_{10}$ CFU for the Δ*dosR-S* strain) in the 5-week experiment (A) and were also not significant in the 8-week experiment (B), in which the doses implanted at day 1 were calculated (calc*) based on the differences between inhaled and implanted doses in the first experiment, which are similar to those reported previously in the literature for the rabbit model (8, 18). For a detailed explanation, see the text. Histopathological analysis of rabbit lungs 5 weeks after infection with *M. tuberculosis* H37Rv (C and E) shows a well-organized primary granulomatous lesion with dark lymphocytes surrounding pale epithelioid macrophages capable of killing tubercle bacilli. In contrast, with the Δ*dosR-S* deletion mutant (D and F), the lesions were fewer and smaller. Magnifications, ×20 (C and D) and ×200 (E and F).

mutant. However, only the wild-type parent and, unexpectedly, neither complemented strain or the deletion mutant expressed Rv3134c (*dosS*). All four strains carried *dosT*, which shares many, if not all, of the functions of DosS (15, 32; data not shown). Therefore, the mutant will be described as Δ*dosR-S*. The complemented strain has a partial restoration of the Rv3134c-Rv3132c operon, as it expresses *dosR* but not *dosS*.

Rabbit infection with the Δ*dosR-S* mutant reveals defective survival. H37Rv Δ*dosR-S* and wild-type parent strains were tested in a 5- and 8-week rabbit aerosol infection model. In the first experiment, both the right upper lobe CFU counts 1 day after aerosol infection and the calculated average inhaled dose were similar for both groups (Fig. 2A). The difference between these two values is the same as that described previously by Lurie in the 1950s (18, 19). The weights, weight gain, and tuberculin skin test results did not differ between groups over the course of the 5-week experiment (Table 1). At week 5, mutant-infected rabbits had slightly smaller right upper lung lobes ($P = 0.05$), consistent with less inflammation, and a trend toward lower total lung weight ($P = 0.08$). However, the total right upper lung lobe CFUs were not significantly

TABLE 1. Differences between rabbits infected with *M. tuberculosis* H37Rv or the Δ*dosR-S* strain at 5 weeks and those infected at 8 weeks after infection in two consecutive experiments

Parameter	Value[b]			
	Wk 5		Wk 8	
	H37Rv	H37Rv:Δ*dosR-S*	H37Rv	H37Rv:Δ*dosR-S*
Tuberculin skin test (mm^3) [median (range)]	62 (7–403)	219 (0–706)	61 (0–4752)	203 (0–960)
Mean hilar lymph node wt (mg) ± SD	423 ± 102	336 ± 52	96 ± 20	92 ± 18
Mean total lung wt (g) ± SD	13.8 ± 1.2	11.2 ± 0.4	13.2 ± 0.8	13.5 ± 0.3
Mean right upper lobe wt (g) ± SD	**1.5 ± 0.2**	**1.2 ± 0.1**[a]	1.0 ± 0.06	1.1 ± 0.04
Mean spleen wt (g) ± SD	2.2 ± 0.4	1.6 ± 0.1	1.7 ± 0.2	1.3 ± 0.1
Avg tubercle count ± SD	187 ± 17	148 ± 44	**113 ± 23**	**27 ± 12**[a]
Avg tubercle diam ± SD	**1.5 ± 0.1**	**1.0 ± 0.1**[a]	1.4 ± 0.2	1.0 ± 0.1

[a] $P \leq 0.05$.
[b] Values in boldface type are statistically significant.

different between the mutant- and wild-type-infected rabbits (Fig. 2A).

In order to assess the possibility of delayed attenuation, a second experiment in which rabbits were sacrificed 8 weeks after aerosol infection was performed (Table 1). At this time point, there was a trend toward lower spleen weights in animals infected with the Δ*dosR-S* strain ($P = 0.06$). The right upper lobe bacillary burden was lower for the mutant than for the wild type ($P = 0.03$), consistent with a lower inoculum but also, possibly, with reduced virulence for the mutant (Fig. 2B). Although the complemented strain was also tested using rabbits, the inhaled dose was significantly lower than that for the other two strains and could not be evaluated. Pathology samples revealed that wild-type-infected lesions appeared more intense, more numerous, and better organized than mutant-infected lesions in the animals sacrificed at 5 weeks (Fig. 2C to F).

We conclude that in the rabbit model, the Δ*dosR-S* mutant induced somewhat less inflammation, was not hypervirulent, and may even have defective survival following the onset of tuberculin reactivity.

Mice resist multiplication of the Δ*dosR-S* strain more effectively than wild-type *M. tuberculosis*. In C57BL/6 mice infected with all three strains, the wild-type strain multiplied normally, while the mutant and Comp strains multiplied more slowly (Fig. 3A and B). By week 4, the CFU counts of the mutant and Comp strains were lower ($P < 0.001$) than those of the wild type in both lungs and spleen. Given the failure of the Comp strain to restore the wild-type phenotype once again even after matching implantation, CFU assessment of this strain was discontinued after week 4. Interestingly, the difference in CFU between the mutant and wild-type strains narrowed between weeks 4 and 16 but remained unchanged at week 24. We conclude that the Δ*dosR-S* mutant does not multiply as well as the wild type in mouse tissues. With matching implantation doses, larger lesions and the pathological involvement of a greater proportion of the lung were observed 2 months after infection in mice infected with the wild-type strain (Fig. 3C) relative to mice infected with the mutant strain (Fig. 3D).

The Δ*dosR-S* mutant is attenuated in guinea pig before onset of tuberculin reactivity. Guinea pigs were aerosol infected in a Madison chamber calculated to deliver ~20 (1.3 $\log_{10}$) CFU/lung of *M. tuberculosis* H37Rv, the Δ*dosR-S* mutant, or the *dosR* complemented strain. By day 14 after infection, growth of nearly 2 $\log_{10}$ CFU/week was found, as expected, in the lungs infected with the wild-type strain to ~10^5 CFU, while fewer than 10^2 CFU and 10^3 CFU were recovered from Δ*dosR-S* strain-infected lungs and complement-infected lungs, respectively (Fig. 4A). At this time point, spleen CFU counts for the complemented strain nearly matched those of the wild-type strain (Fig. 4A). By week 6, wild-type-infected lung and spleen CFU counts were higher than the corresponding CFU counts at day 14. Although organ CFU counts for the mutant and complemented strains were also higher than their respective day 14 values, they remained low relative to the corresponding organ CFU for the wild type at 6 weeks. Skin test responses at week 6 were comparable for wild-type- and complement-infected guinea pigs and significantly greater ($P < 0.025$) than that of the mutant-infected animals (Fig. 4B). These results are consistent with a growth defect for the Δ*dosR-S* mutant in guinea pig organs but also with a reduced virulence of the complemented strain in this model.

Two weeks after infection, relatively small tubercles could be seen in wild-type-infected guinea pig lungs (Fig. 5A), with early granulomatous lesions seen at higher magnifications (Fig. 5G). Conversely, at the same time point, there was little inflammation in the lungs of guinea pigs infected with either the mutant (Fig. 5B) or complemented (Fig. 5C) strain, with only a few scattered inflammatory cells (Fig. 5H). By 6 weeks, there was massive inflammation in wild-type-infected lungs (Fig. 5D), and lesions revealed extensive central necrosis (Fig. 5I). Inflammation appeared to be reduced in Δ*dosR-S* strain-infected lungs (Fig. 5E), with a lack of mature granuloma formation and minimal necrosis (Fig. 5J) relative to lesions in complement-infected animals (Fig. 5F), consistent with a reduced virulence of the Δ*dosR-S* mutant.

Finally, we attempted to quantify both the lesion number and the percentage of the lung sections occupied by granulomas for each strain. These data are shown in Table S2 in the supplemental material. In general, lesion number and percentage of lung occupied by granulomas correlated very well, with the exception of one mutant-infected animal and one complement-infected animal. A qualitative analysis of these exceptions indicated that their granulomas were poorly formed, abortive, or immature lesions that in no way resembled the lesions seen in the wild-type-infected animals.

In the mouse HF model of latent tuberculosis, the *dosR* and *dosS* genes are not essential for *M. tuberculosis* persistence. The mouse HF model facilitates the establishment of *M. tuber-*

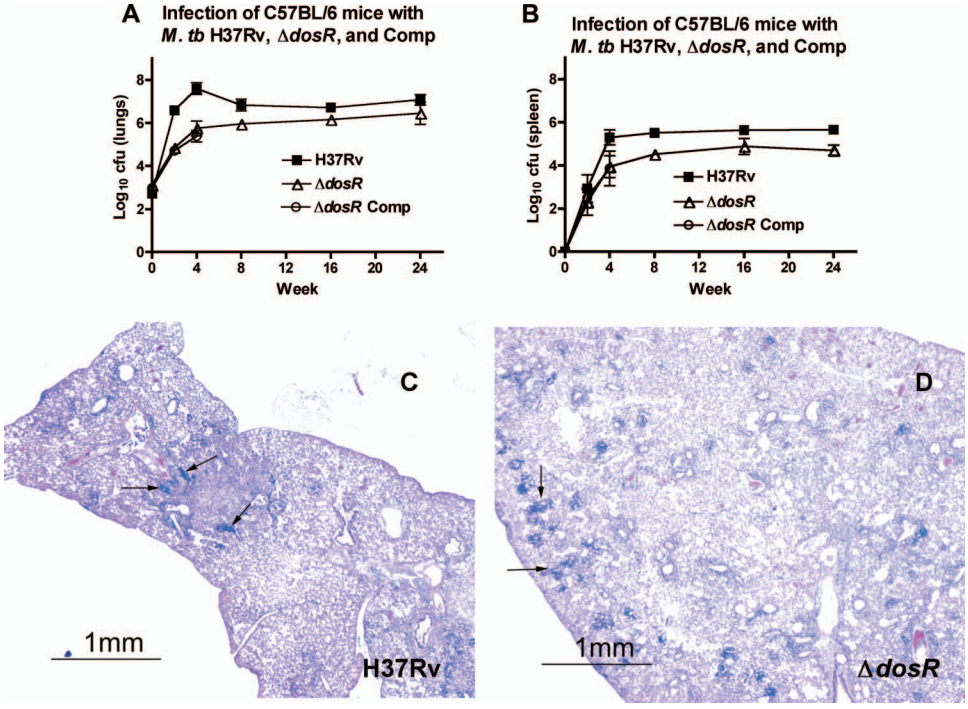

FIG. 3. Growth after well-matched implantation of wild-type H37Rv, Δ*dosR-S*, and Comp strains. In spite of comparable implantation levels, the Δ*dosR-S* mutant did not multiply as well in the lungs (A) or the spleen (B) as the wild type. The Δ*dosR-S* mutant complemented with the mycobacterial optimal promoter (Comp) does not grow as well in the lungs or spleen as the wild-type strain even with comparable levels of implantation (2.71 ± 0.19 $\log_{10}$ CFU for H37Rv, 3.11 ± 0.11 $\log_{10}$ CFU for the Δ*dosR-S* strain, and 2.98 ± 0.20 $\log_{10}$ CFU for Comp) over the first 28 days. (C and D) Histopathology of lungs of C57BL/6 mice infected with *M. tuberculosis* (*M. tb*) H37Rv (C) or a Δ*dosR-S* deletion mutant (D) 2 months after infection. At 2 months, the lesions were large and dense in wild-type-infected mouse lungs compared to the scattered lesions in Δ*dosR-S*-infected mouse lungs, in which more normal lung tissue was preserved. No lesions showed evidence of necrosis. Magnification, ×20.

culosis persistence in an extracellular, paucibacillary state analogous to that for solid caseous necrosis. *M. tuberculosis* cells encapsulated within semidiffusible HFs implanted in mice demonstrate a phenotype characterized by stationary-state CFU, decreased metabolic activity, and increased susceptibility to the sterilizing drug rifampin compared to the bactericidal drug isoniazid (12). Recently, the hypoxia-specific marker pimonidazole was shown to stain the perifiber granulomatous tissue in this model in a bacillary dose-dependent manner (14), suggesting that hypoxia may play a role in intrafiber bacillary growth containment.

Mice gained weight equivalently in the three groups over 56 days (not shown). Spleen weights increased in mice implanted with fibers containing Comp over the first 14 days, but all mice had similar spleen weights by day 56 (not shown).

Intrafiber CFU counts remained stable over 56 days. On day

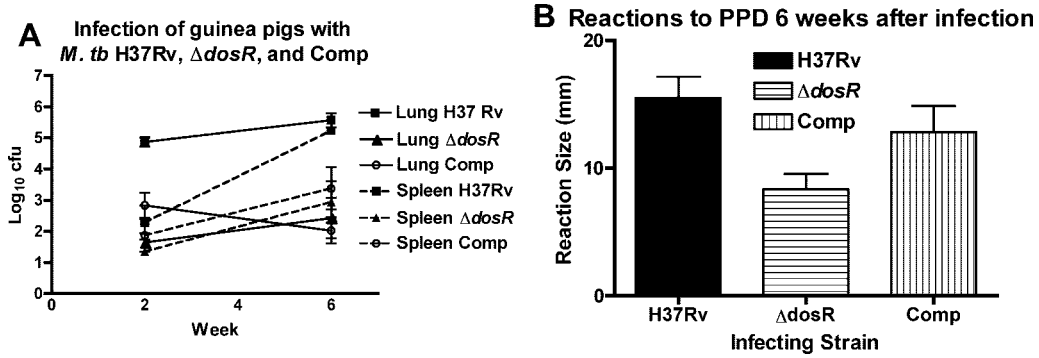

FIG. 4. Guinea pigs resist multiplication of *M. tuberculosis* (*M. tb*) cells lacking *dosR* and *dosS*. (A) After infection with approximately 1.3 $\log_{10}$ CFU, the complemented strain (Comp) initially multiplied at an intermediate level between H37Rv wild-type and Δ*dosR-S* mutant bacillus levels before the onset of tuberculin reactivity, but by week 6, the growth of this strain declined to the same level as that seen for the Δ*dosR-S* mutant bacilli. Lungs are shown with solid lines, and spleens are shown with dashed lines. (B) Reactivity to tuberculin (PPD). The wild-type and complemented (Comp) strains elicit a stronger ($P < 0.025$ by one-way analysis of variance) mean delayed-type hypersensitivity response to PPD than does the Δ*dosR-S* mutant (horizontal stripes).

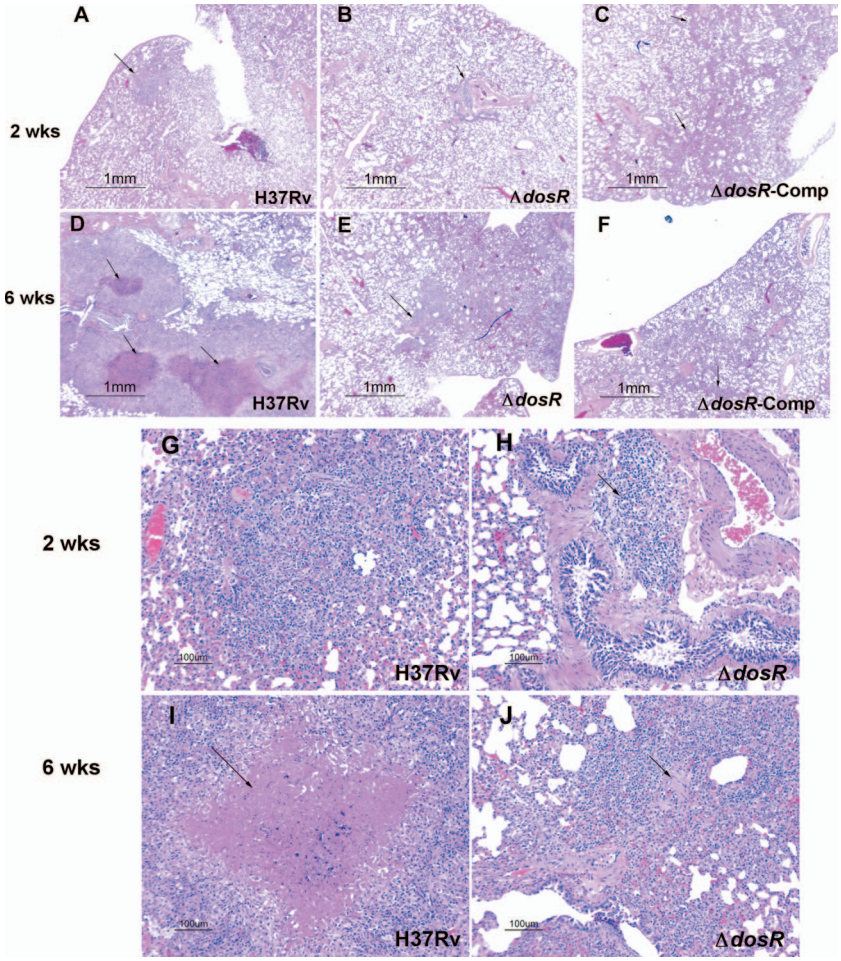

FIG. 5. (A to C) Histopathology of lungs of guinea pigs infected with *M. tuberculosis* H37Rv, a Δ*dosR-S* deletion mutant, or the mutant complemented with *dosR* at 2 weeks, before the onset of tuberculin reactivity. Only a small early granulomatous, noncaseating lesion (arrow) in the lung of a wild-type-infected guinea pig was observed at this time (A). Mutant- and complement-infected guinea pigs showed only rare inflammatory peribronchial/periarteriolar infiltrates (arrows). (D to F) At 6 weeks, there was strong tuberculin reactivity (see Table S2 in the supplemental material) and substantial inflammation and necrosis (arrows) in the lungs of wild-type-infected guinea pigs (D), almost none detectable in the mutant-infected animals (E), and small, poorly organized granulomas (arrows) in the complement-infected guinea pigs (F). Magnification, ×20. (G to J) Above-described lung lesions of guinea pigs infected with H37Rv wild-type (G and I) and Δ*dosR-S* (H and J) mutant strains at higher magnifications. Caseous necrosis (arrow) is apparent in the lesions of the wild-type-infected guinea pig at 6 weeks (I), whereas a rare lesion (J) in a Δ*dosR-S* mutant-infected animal shows rather poor organization and limited necrosis (arrow). Magnification, ×100.

1 after HF implantation, counts varied between 300 and 1,000 CFU per fiber for each of the three groups. As observed previously (12, 14), numbers of wild-type CFU remained relatively constant throughout. Although the Δ*dosR-S* strain appeared to have an initial intrafiber survival defect, since CFU decreased by 10-fold on day 14 after fiber implantation, CFU counts at day 56 were not statistically significantly different than those on day 1 (not shown). Interestingly, Comp did not appear to have an intrafiber survival defect during the first 14 days after HF implantation, but CFU counts declined more than 10-fold by day 28 and remained statistically significantly lower than those of the other two groups at day 56 after fiber implantation ($P < 0.05$).

As observed previously (12), HFs containing wild-type *M. tuberculosis* cells progressively developed thick, circumferential inflammation in the subcutaneous tissue immediately surrounding the HF. The perifiber pathologies, both grossly and histologically (not shown), were similar in wild-type-, Δ*dosR-S* mutant-, and complement-containing fibers. Taken together, the results for the HF model indicate that there is neither increased virulence nor attenuation of the Δ*dosR-S* strain compared to the wild type.

DISCUSSION

NO, the predominant mechanism limiting bacillary growth in mouse lungs (5, 20), and hypoxia, prevalent in the caseous and necrotic lesions of guinea pigs (17) and rabbits (38), both induce DosR and its regulon (33, 34, 39). Contrary to previous studies reporting hypervirulence of a *dosR*-deficient mutant in DBA/2 mice (26), our data suggest that disruption of *dosR* leads to attenuation in a mouse aerosol model using the more resistant BALB/c (data not shown) and C57BL/6 mouse strains. Consistent with previously reported findings (21), our

mutant was also attenuated in the guinea pig model. Since the rabbit is relatively resistant to *M. tuberculosis* infection (8, 22), a hypervirulent mutant should be readily apparent in this model. However, such a phenotype was not observed in our study, suggesting that a *dosR* deficiency does not lead to increased virulence in vivo.

We observed the failure of the *dosR*-complemented strain to restore the wild-type phenotype. This finding may be explained by the fact that *dosR* appears to be the second gene in an operon: Rv3134c, Rv3133c (*devR*, or *dosR*), and Rv3132c (*devS*, or *dosS*). In such a location, disruption of *dosR* may have a polar effect on the expression of the distal gene *dosS*. Indeed, *dosS* expression was not restored in the complement strain, suggesting a potential role for *dosS* in the observed attenuated phenotype of this strain. The possibility of polar effects occurring downstream of mutations in this operon was also suggested in a recent study in which an Rv3134c transposon mutant was attenuated in different models of hypoxia (14). Given the lack of complete data on complemented *dosR* strains in previous reports, the possibility remains that complementation in *trans* may result in inappropriately regulated expression and a reduction of viability (35).

The discrepancy between our findings, those of Rustad et al. (31), and those of Parish et al. (26) might be explained by mismatched implantation in the latter study, since lung CFU counts at day 1 were not reported, and the difference between mutant and wild-type groups in lung CFU counts at day 15 became progressively smaller through day 60. In our study, with matching CFU burdens in C57BL/6 mice on day 1, the mutant was found to be attenuated with respect to both lung CFU burden and immunopathology. No mortality was observed out to 24 weeks. This finding underscores the importance of assessing lung implantation CFU counts when comparing the in vivo growth levels of *M. tuberculosis* strains.

The immunological mechanisms by which the multiplication of *M. tuberculosis* infection is contained vary between species. In rabbit, guinea pig, monkey, and human tuberculosis, there is caseous necrosis at the center of lesions (38), in which the bacilli are rare and do not grow. In the mouse, there is no caseous necrosis, and bacillary proliferation is controlled by other means (1, 13). Necrotic human tuberculous lesions may be hypoxic, and there is evidence suggesting that the lesions are not vascularized (36) in other species, whereas in the mouse, the lesions display abundant endothelial cells and vascularization (2). Mouse macrophages can be induced by gamma interferon (IFN-γ) or tumor necrosis factor alpha (TNF-α) to produce NO, which is lethal for tubercle bacilli. The inhibition of NO production chemically or genetically enhances bacillary proliferation in mice (5, 20). On the other hand, the IFN-γ-mediated induction of NO in rabbit, guinea pig, and human monocytes/macrophages in vitro has been difficult to show (11, 25). Both mechanisms have lethal effects on tubercle bacilli (4), and both mechanisms induce DosR and its regulon (33, 34, 39). We found that crippling of this mechanism did not enhance the ability of the bacilli to proliferate in mice, which use the NO route of containment, or in guinea pigs and rabbits, which may or may not use NO but certainly have caseous necrosis and hypoxic granulomas (17, 38). Instead, an inability to make a major adaptive response to hypoxia and NO resulted in diminished levels of growth after high levels of NO, TNF-α, and IFN-γ are achieved in mice by week 2 (20) and the onset of caseous necrosis in rabbit and guinea pig lungs (Fig. 2 and 5).

A limitation of our studies is the lack of cytokine data that might contribute to a better understanding of the host immune response to attenuated *M. tuberculosis* mutants. Previous studies of sigma factor Δ*sigH* (13) and Δ*sigC* (1) mutants, which have an immunopathology phenotype characterized by significantly reduced inflammatory lesions in mice despite lung bacillary loads comparable to those achieved by wild-type *M. tuberculosis*, showed that this attenuated phenotype is associated with lower levels of TNF-α and IFN-γ at certain time points after infection. However, most cytokine analyses of attenuated *M. tuberculosis* strains have been done using macrophage models (30) rather than animal organs, again revealing reduced Th1-type immune responses. Given the attenuated phenotype observed in our studies, we predict a similar pattern of reduced levels of proinflammatory cytokines induced by the Δ*dosR-S* mutant.

Differences in the observed in vivo phenotypes of *dosR*-deficient *M. tuberculosis* between our study and previously published reports (21, 26) may also be explained by differences in mutant generation. Parish et al. deleted the central 447 bp between BalI sites of *dosR* without a drug resistance replacement cassette (26), whereas our mutant lacks all but the most distal 19 bp of *dosR* and contains a kanamycin-resistance cassette. The kanamycin cassette inserted by Malhotra et al. (21) left intact a region capable of encoding the first 145 N-terminal amino acids of DosR and lacking only the 72-amino-acid C-terminal domain. Although it is unclear why the two mutants which lack most or all of the 3′ coding region are attenuated, it is possible that the deletion of this region disrupts the expression of *dosS*. Therefore, it would be worthwhile to test for *dosS* expression in the other two mutants.

The phenotypes of *M. tuberculosis* strains have been characterized primarily in terms of growth patterns and secondarily in terms of murine host responses (10). Our Δ*dosR-S* mutant displayed a range of phenotypes in the various animal models tested. Despite limited data, the Δ*dosR-S* mutant appeared to exhibit a persistence (*per*) phenotype, such as Δ*icl* (24), in the rabbit model, and a growth-in-vivo (*giv*) phenotype, such as Δ*phoP* (27), in the guinea pig model. In the mouse model, when implantation doses of mutant and wild-type strains were matched, the growth kinetics of the mutant were again consistent with a *giv* phenotype. Therefore, depending on immune as well as physicochemical factors stressing the organism, such as NO and hypoxia, the Δ*dosR-S* mutant exhibits varied phenotypes either no different from or attenuated relative to that of the wild type. These observations support the concept that bacterial phenotypes are both dose and host dependent.

By testing *M. tuberculosis* mutants in different animal models, we more robustly assess gene function because of the different conditions present in these models. Genes and their products, which are potential drug or vaccine targets, may function very differently in the intracellular compartments typically found in the mouse compared to the necrotic caseum in rabbit or guinea pig lesions.

ACKNOWLEDGMENTS

We gratefully acknowledge the support of NIAID NO1 30036, R01 36973, R0137856, and R01 43846 and a senior scholar award from the Ellison Medical Foundation.

We also thank David R. Sherman and his laboratory at the University of Washington for the strains used in these experiments and for the details of their construction. We thank Arthur M. Dannenberg, Jr., for advice on rabbit histopathology. We thank Sandeep Tyagi and Kathy Williams for assistance with the mouse experiments.

REFERENCES

1. **Abdul-Majid, K.-B., L. Ly, P. Converse, D. Geiman, D. McMurray, and W. Bishai.** 2008. Altered cellular infiltration and cytokine levels during early *Mycobacterium tuberculosis sigC* mutant infection are associated with late-stage disease attenuation and milder immunopathology in mice. BMC Microbiol. **8:**151.
2. **Aly, S., K. Wagner, C. Keller, S. Malm, A. Malzan, S. Brandau, F. C. Bange, and S. Ehlers.** 2006. Oxygen status of lung granulomas in *Mycobacterium tuberculosis*-infected mice. J. Pathol. **210:**298–305.
3. **Boon, C., and T. Dick.** 2002. *Mycobacterium bovis* BCG response regulator essential for hypoxic dormancy. J. Bacteriol. **184:**6760–6767.
4. **Boshoff, H. I. M., and C. E. Barry.** 2005. Tuberculosis metabolism and respiration in the absence of growth. Nat. Rev. Microbiol. **3:**70–80.
5. **Chan, J., K. Tanaka, D. Carroll, J. Flynn, and B. R. Bloom.** 1995. Effects of nitric oxide synthase inhibitors on murine infection with *Mycobacterium tuberculosis*. Infect. Immun. **63:**736–740.
6. **Converse, P. J., A. M. Dannenberg, Jr., J. E. Estep, K. Sugisaki, Y. Abe, B. H. Schofield, and M. L. Pitt.** 1996. Cavitary tuberculosis produced in rabbits by aerosolized virulent tubercle bacilli. Infect. Immun. **64:**4776–4787.
7. **Dannenberg, A. M., Jr.** 1998. Lurie's tubercle-count method to test TB vaccine efficacy in rabbits. Front. Biosci. **3:**27–33.
8. **Dannenberg, A. M., Jr.** 2006. Pathogenesis of human pulmonary tuberculosis: insights from the rabbit model. ASM Press, Washington, DC.
9. **George, K. M., Y. Yuan, D. R. Sherman, and C. E. Barry III.** 1995. The biosynthesis of cyclopropanated mycolic acids in *Mycobacterium tuberculosis*. J. Biol. Chem. **270:**27292–27298.
10. **Hingley-Wilson, S. M., V. K. Sambandamurthy, and W. R. Jacobs, Jr.** 2003. Survival perspectives from the world's most successful pathogen, *Mycobacterium tuberculosis*. Nat. Immunol. **4:**949–955.
11. **Jeevan, A., C. T. McFarland, T. Yoshimura, T. Skwor, H. Cho, T. Lasco, and D. N. McMurray.** 2006. Production and characterization of guinea pig recombinant gamma interferon and its effect on macrophage activation. Infect. Immun. **74:**213–224.
12. **Karakousis, P. C., T. Yoshimatsu, G. Lamichhane, S. C. Woolwine, E. L. Nuermberger, J. Grosset, and W. R. Bishai.** 2004. Dormancy phenotype displayed by extracellular *Mycobacterium tuberculosis* within artificial granulomas in mice. J. Exp. Med. **200:**647–657.
13. **Kaushal, D., B. G. Schroeder, S. Tyagi, T. Yoshimatsu, C. Scott, C. Ko, L. Carpenter, J. Mehrotra, Y. C. Manabe, R. D. Fleischmann, and W. R. Bishai.** 2002. Reduced immunopathology and mortality despite tissue persistence in a *Mycobacterium tuberculosis* mutant lacking alternative sigma factor, SigH. Proc. Natl. Acad. Sci. USA **99:**8330–8335.
14. **Klinkenberg, L. G., L. A. Sutherland, W. R. Bishai, and P. C. Karakousis.** 2008. Metronidazole lacks activity against *Mycobacterium tuberculosis* in an in vivo hypoxic granuloma model of latency. J. Infect. Dis. **198:**275–283.
15. **Kumar, A., J. C. Toledo, R. P. Patel, J. R. Lancaster, Jr., and A. J. C. Steyn.** 2007. *Mycobacterium tuberculosis* DosS is a redox sensor and DosT is a hypoxia sensor. Proc. Nat. Acad. Sci. USA **104:**11568–11573.
16. **Lecoeur, H. F., P. H. Lagrange, C. Truffot-Pernot, M. Gheorghiu, and J. Grosset.** 1989. Relapses after stopping chemotherapy for experimental tuberculosis in genetically resistant and susceptible strains of mice. Clin. Exp. Immunol. **76:**458–462.
17. **Lenaerts, A. J., D. Hoff, S. Aly, S. Ehlers, K. Andries, L. Cantarero, I. M. Orme, and R. J. Basaraba.** 2007. Location of persisting mycobacteria in a guinea pig model of tuberculosis revealed by R207910. Antimicrob. Agents Chemother. **51:**3338–3345.
18. **Lurie, M. B., S. Abramson, and A. G. Heppleston.** 1952. On the response of genetically resistant and susceptible rabbits to the quantitative inhalation of human-type tubercle bacilli and the nature of resistance to tuberculosis. J. Exp. Med. **95:**119–134.
19. **Lurie, M. B., A. G. Heppleston, S. Abramson, and I. B. Swartz.** 1950. Evaluation of the method of quantitative airborne infection and its use in the study of the pathogenesis of tuberculosis. Am. Rev. Tuberc. **61:**765–797.
20. **MacMicking, J. D., R. J. North, R. LaCourse, J. S. Mudgett, S. K. Shah, and C. F. Nathan.** 1997. Identification of nitric oxide synthase as a protective locus against tuberculosis. Proc. Natl. Acad. Sci. USA **94:**5243–5248.
21. **Malhotra, V., D. Sharma, V. D. Ramanathan, H. Shakila, D. K. Saini, S. Chakravorty, T. K. Das, Q. Li, R. F. Silver, P. R. Narayanan, and J. S. Tyagi.** 2004. Disruption of response regulator gene, *devR*, leads to attenuation in virulence of *Mycobacterium tuberculosis*. FEMS Microbiol. Lett. **231:**237–245.
22. **Manabe, Y. C., A. M. Dannenberg, Jr., S. K. Tyagi, C. L. Hatem, M. Yoder, S. C. Woolwine, B. C. Zook, M. L. Pitt, and W. R. Bishai.** 2003. Different strains of *Mycobacterium tuberculosis* cause various spectrums of disease in the rabbit model of tuberculosis. Infect. Immun. **71:**6004–6011.
23. **Manganelli, R., E. Dubnau, S. Tyagi, F. R. Kramer, and I. Smith.** 1999. Differential expression of 10 sigma factor genes in *Mycobacterium tuberculosis*. Mol. Microbiol. **31:**715–724.
24. **McKinney, J. D., K. H. zu Bentrup, E. J. Munoz-Elias, A. Miczak, B. Chen, W.-T. Chan, D. Swenson, J. C. Sacchettini, W. R. Jacobs, and D. G. Russell.** 2000. Persistence of *Mycobacterium tuberculosis* in macrophages and mice requires the glyoxylate shunt enzyme isocitrate lyase. Nature **406:**735–738.
25. **Nathan, C., P. Liu, J. S. Adams, and R. L. Modlin.** 2006. Role of iNOS in human host defense. Science **312:**1874–1875.
26. **Parish, T., D. A. Smith, S. Kendall, N. Casali, G. J. Bancroft, and N. G. Stoker.** 2003. Deletion of two-component regulatory systems increases the virulence of *Mycobacterium tuberculosis*. Infect. Immun. **71:**1134–1140.
27. **Perez, E., S. Samper, Y. Bordas, C. Guilhot, B. Gicquel, and C. Martin.** 2001. An essential role for *phoP* in *Mycobacterium tuberculosis* virulence. Mol. Microbiol. **41:**179–187.
28. **Roach, D. R., H. Briscoe, B. Saunders, M. P. France, S. Riminton, and W. J. Britton.** 2001. Secreted lymphotoxin-alpha is essential for the control of an intracellular bacterial infection. J. Exp. Med. **193:**239–246.
29. **Roberts, D. M., R. P. Liao, G. Wisedchaisri, W. G. Hol, and D. R. Sherman.** 2004. Two sensor kinases contribute to the hypoxic response of *Mycobacterium tuberculosis*. J. Biol. Chem. **279:**23082–23087.
30. **Russell-Goldman, E., J. Xu, X. Wang, J. Chan, and J. M. Tufariello.** 2008. A *Mycobacterium tuberculosis* Rpf double-knockout strain exhibits profound defects in reactivation from chronic tuberculosis and innate immunity phenotypes. Infect. Immun. **76:**4269–4281.
31. **Rustad, T. R., M. I. Harrell, R. Liao, and D. R. Sherman.** 2008. The enduring hypoxic response of *Mycobacterium tuberculosis*. PLoS ONE **3:**e1502.
32. **Saini, D. K., V. Malhotra, and J. S. Tyagi.** 2004. Cross talk between DevS sensor kinase homologue, Rv2027c, and DevR response regulator of *Mycobacterium tuberculosis*. FEBS Lett. **565:**75–80.
33. **Schnappinger, D., S. Ehrt, M. I. Voskuil, Y. Liu, J. A. Mangan, I. M. Monahan, G. Dolganov, B. Efron, P. D. Butcher, C. Nathan, and G. K. Schoolnik.** 2003. Transcriptional adaptation of *Mycobacterium tuberculosis* within macrophages: insights into the phagosomal environment. J. Exp. Med. **198:**693–704.
34. **Sherman, D. R., M. Voskuil, D. Schnappinger, R. Liao, M. I. Harrell, and G. K. Schoolnik.** 2001. Regulation of the *Mycobacterium tuberculosis* hypoxic response gene encoding alpha-crystallin. Proc. Natl. Acad. Sci. USA **98:**7534–7539.
35. **Stewart, G. R., V. A. Snewin, G. Walzl, T. Hussell, P. Tormay, P. O'Gaora, M. Goyal, J. Betts, I. N. Brown, and D. B. Young.** 2001. Overexpression of heat-shock proteins reduces survival of *Mycobacterium tuberculosis* in the chronic phase of infection. Nat. Med. **7:**732–737.
36. **Tsai, M. C., S. Chakravarty, G. Zhu, J. Xu, K. Tanaka, C. Koch, J. Tufariello, J. Flynn, and J. Chan.** 2006. Characterization of the tuberculous granuloma in murine and human lungs: cellular composition and relative tissue oxygen tension. Cell. Microbiol. **8:**218–232.
37. **Turner, O. C., R. J. Basaraba, and I. M. Orme.** 2003. Immunopathogenesis of pulmonary granulomas in the guinea pig after infection with *Mycobacterium tuberculosis*. Infect. Immun. **71:**864–871.
38. **Via, L. E., P. L. Lin, S. M. Ray, J. Carrillo, S. S. Allen, S. Y. Eum, K. Taylor, E. Klein, U. Manjunatha, J. Gonzales, E. G. Lee, S. K. Park, J. A. Raleigh, S. N. Cho, D. N. McMurray, J. L. Flynn, and C. E. Barry III.** 2008. Tuberculous granulomas are hypoxic in guinea pigs, rabbits, and nonhuman primates. Infect. Immun. **76:**2333–2340.
39. **Voskuil, M. I., D. Schnappinger, K. C. Visconti, M. I. Harrell, G. M. Dolganov, D. R. Sherman, and G. K. Schoolnik.** 2003. Inhibition of respiration by nitric oxide induces a *Mycobacterium tuberculosis* dormancy program. J. Exp. Med. **198:**705–713.
40. **Wayne, L. G., and L. G. Hayes.** 1996. An in vitro model for sequential study of shiftdown of *Mycobacterium tuberculosis* through two stages of nonreplicating persistence. Infect. Immun. **64:**2062–2069.
41. **Wiegeshaus, E. H., D. N. McMurray, A. A. Grover, G. E. Harding, and D. W. Smith.** 1970. Host-parasite relationships in experimental airborne tuberculosis. 3. Relevance of microbial enumeration to acquired resistance in guinea pigs. Am. Rev. Respir. Dis. **102:**422–429.

Editor: W. A. Petri, Jr.